OXFORD

Carcinogenesis, 2015, Vol. 36, No. 3, 378–389

doi:10.1093/carcin/bgu323
Advance Access publication January 2, 2015
Original Manuscript

ORIGINAL MANUSCRIPT

Rac1 promotes diethylnitrosamine (DEN)-induced formation of liver tumors

Anita Bopp[1,†], Friedrich Wartlick[1,†], Christian Henninger[1], Michael Schwarz[3], Bernd Kaina[2] and Gerhard Fritz[1,*]

[1]Institute of Toxicology, Heinrich Heine University Düsseldorf, Moorenstrasse 5, D-40225 Düsseldorf, Germany, [2]Institute of Toxicology, University Medical Center Mainz, Obere Zahlbacher Str. 67, D-55131 Mainz, Germany and [3]Institute of Pharmacology and Toxicology, University Tübingen, Wilhelmstrasse 76, D-72074 Tübingen, Germany

*To whom correspondence should be addressed. Tel: +49 211 8113022; Fax: +49 211 813013; Email: fritz@uni-duesseldorf.de
†These authors contributed equally to this work.

Abstract

To elucidate the function of the Ras-homologous GTPase Rac1 in hepatocarcinogenesis induced by diethylnitrosamine (DEN), mice lacking hepatic Rac1 expression were treated with DEN and compared to the wild-type (WT). Rac1 knock-out (KO) mice were found to have a lower tumor yield as compared to Rac1 proficient mice. The small-sized tumors formed in the absence of Rac1 lack an activated Ras/Raf/mitogen-activated protein kinase pathway, as indicated by the absence of *p*-ERK expression. Apparently, Rac1 is required for Ras-driven oncogenic pathways. Moreover, tumors in Rac1 deficient mice were glutamine synthase (GS) negative. They displayed a high number of *p*-H3-positive and cyclinB1 expressing cells, pointing to a defect in mitotic progression. To elucidate the influence of Rac1 on mechanisms of tumor initiation, acute DEN-induced hepatic stress responses were monitored. Rac1 deficiency caused fairly complex, partially time-dependent, alterations in both basal and/or DEN-induced messenger RNA (mRNA) and protein levels of susceptibility-related genes. Basal protein expression of DNA repair factors Brca1 and DNA repair protein RAD51 homolog (Rad51) and the cell cycle regulatory factor p27 was enhanced in the absence of Rac1. Following DEN treatment, p21 mRNA and protein expression was stimulated independent of the Rac1 status. Lack of Rac1 increased mechanisms of the DNA damage response (DDR), as shown by elevated protein levels of *p*-ATR, *p*-p53 and γH2AX 24 h after DEN treatment. The data show that Rac1 is essential for DEN-stimulated hepatocarcinogenesis. We hypothesize that it promotes tumor initiation by counteracting the elimination of initiated cells and, moreover, alleviates the outgrowth of transformed cells. Hence, pharmacological targeting of Rac1 could be suitable for chemoprevention.

Introduction

Rac1 belongs to the family of low molecular weight Ras-homologous (Rho) GTPases, which play a key role in the regulation of numerous cellular processes (1,2). Rac1 controls cell-cell adhesion and epithelial-mesenchymal transition (3), regulates mitosis and meiosis (4,5), cross-talks with oncogenes important for the development of acute myeloid leukemia (6,7), regulates B-cell development and signaling (8), impacts cell spreading and membrane ruffling (9) and is required for Ras-mediated transformation (10). Moreover, it is a key regulator of stress-activated protein kinases (SAPK/JNK), p38 kinase (11,12) and of a broad spectrum of transcription factors including c-Jun, ATF2, NF-κB and Smad proteins (13–15). Due to the key functions of Rho GTPases in the pathophysiology of malignant diseases, pharmacological targeting of Rho proteins was suggested as effective strategy to improve anticancer therapy (16). One promising therapeutic option to influence Rho signaling are HMG-CoA reductase inhibitors (statins), which are widely used in the clinic for lipid lowering purpose. They interfere with Rho signaling by depleting the cellular pool of isoprene precursor molecules, which are essential for correct intracellular localization

Received: March 20, 2014; **Revised:** December 22, 2014; **Accepted:** December 24, 2014

Abbreviations:

Alb	albumin
Cre	cyclization recombinase
DDR	DNA damage response
DEN	diethylnitrosamine
DSB	DNA double-strand breaks
ERK	extracellular regulated kinase
GAPDH	glyceraldehyde 3-phosphate dehydrogenase
GS	glutamine synthase
H&E	hematoxylin and eosin stain
JNK	c-Jun-N-terminal kinase
KO	knock-out
MGMT	O^6-methylguanin-DNA-methyltransferase
MPO	myeloperoxidase
mRNA	messenger RNA
p-H3	S10 phosphorylated histone H3
qRT–PCR	quantitative reverse transcriptase polymerase chain reaction
Rad51	DNA repair protein RAD51 homolog
Rho	Ras-homologous
TUNEL	terminal deoxynucleotidyl transferase-mediated dUTP nick end labeling
WT	wild-type

and function of Rho GTPases (17). Noteworthy, statins reduce the incidence of mammary tumors resulting from irradiation (18) and protect from dimethylhydrazin-induced colon carcinogenesis (19). Moreover, statins have been suggested as chemopreventive strategy in hepatocellular carcinoma (20). RhoA and Rac1 are considered as the most relevant targets of statins (21). In line with this, pharmacological inhibition of Rac1 signaling by statins or small-molecule inhibitors attenuate metastatic processes in mice (22).

Despite the bulk of *in vitro* data suggesting a pivotal role of Rac1 in controlling mechanisms associated with tumor development, the relevance of Rac1 for chemical carcinogenesis has not yet been reappraised under complex *in vivo* situation. Bearing in mind the prevalence of Ras in human malignancies, it is important to understand the contribution of Ras downstream pathways, such as Rac1-regulated mechanisms, for transformation and tumor progression. Recently it has been observed that Rac1 is required for early changes in the development of pancreatic cancer (23) and is essential for K-Ras-induced lung cancer (24). Moreover Rac1 is required for K-Ras driven epithelial cell hyperproliferation (25) and crucial for skin tumor formation (26). In line with this, mice deficient in the Rac1 activator Tiam-1 are resistant to Ras-induced formation of skin tumors (27). In the present study we investigated the influence of Rac1 on the formation of liver tumors following treatment of wild-type (WT) and *rac1* knock-out (KO) mice with a single dose of the alkylating carcinogen *N*-diethyl-*N*-nitrosamine (DEN). Because of the early embryonic lethality (day e6.5 of development) of systemic *rac1* KO (28), which is due to impaired formation of the three germ layers during gastrulation, we bred $Rac1^{flox/flox}$ with mice albumin-cyclization recombinase (Alb-Cre) transgenic animals. The progeny ($Rac1^{flox/flox/Alb\text{-}Cre}$) is characterized by a liver specific, Alb promotor-driven expression of the Cre recombinase, leading to a KO of the *rac1* gene in hepatocytes. Moreover, to specifically elucidate the impact of Rac1 signaling on mechanisms related to tumor initiation, we thoroughly investigated acute hepatic stress responses, in particular the DNA damage response (DDR), and induction of apoptosis following DEN treatment. The data obtained show that Rac1 deficiency considerably reduces hepatocarcinogenesis and has fairly complex effects on acute DEN-induced hepatic stress responses. The data show that Rac1 influences processes of both tumor initiation and promotion, indicating that it plays a key role in DEN-stimulated hepatocarcinogenesis.

Materials and methods

Mouse experiments

Mice were bred in the local animal facility of the University Medical Center Mainz (Germany) and received humane care according to the criteria outlined in the 'Guide for the Care and Use of Laboratory animals'. $Rac1^{flox/flox}$ mice with a C57BL/6 background (8) were crossed with C57BL/6 mice expressing the Cre recombinase under control of the Alb promotor (Alb-Cre mice). The Alb-driven Cre recombination already occurs in fetal and neonatal mice (29) and further progresses with age (30). The resulting *rac1* KO progeny was comparatively analyzed with transgenic $Rac^{flox/flox}$ WT mice regarding their acute hepatic stress responses following a single treatment with DEN [90 mg/kg BW, intraperitoneal (i.p.) analysis 24 h and 72 h after treatment]. 90 mg/kg BW of DEN is effective in triggering substantial stress responses, and therefore is frequently used in hepatotoxicity studies in rodents. Animals aged 10–12 weeks were used for these studies (group size 3–6 animals). To investigate chemical hepatocarcinogenesis, animals aged 2–3 weeks were exposed to a single dose of DEN (10 mg/kg BW, i.p.). Exposure of young animals to 10 mg/kg BW of DEN is a frequently used approach to achieve a highly efficient induction of liver tumors (31–33). The formation of liver tumors was analyzed 40 weeks later. Here, the group size was $n = 14$ and $n = 18$ animals for *rac1* KO and WT animals, respectively. At the end of the experiments, liver was either fixed in 4.5% paraformaldehyde for subsequent (immuno) histochemical analyses or was frozen in liquid nitrogen for biochemical analyses.

Preparation of DNA and genomic PCR analysis

Genomic DNA from liver was isolated using the DNeasy Blood & Tissue Kit (Qiagen, Hilden, Germany). PCR reactions were performed using RED Taq ReadyMix (Sigma Aldrich, Steinheim) and specific primers (each 0.45 µM; designed by use of Primer3 software), which allows the confirmation of the *rac1* gene KO (primer sequence see Supplementary Table 1, available at *Carcinogenesis* Online). After initial denaturation step (95°C, 2 min), 30 cycles were performed (95°C, 30 s; 55°C, 30 s; 72°C, 45 s). To terminate the reaction, samples were incubated at 72°C for 10 min. PCR products were separated by gel electrophoresis (1.4% agarose gels) and visualized by ethidium bromide staining.

qRT–PCR analysis

To purify total messenger RNA (mRNA) from liver, the RNeasy Mini Kit (Qiagen, Hilden, Germany) was used. RNA was isolated from the liver of $n = 3$–6 animals per group and pooled for complementary DNA synthesis using the OmniScript Kit (Qiagen, Hilden, Germany). For each reaction 2000 ng of total mRNA was applied. For quantitative real-time PCR analysis, the SensiMix SYBR & Fluorescein Kit (Bioline, London, UK) and a MyIQ Thermal Cycler (BioRad, Munich, Germany) were used. The reactions were performed with 40 ng of complementary DNA (1:10 dilution) and specific primers (250 nM) according to the following protocol: 95°C, 10 min; 45 cycles of 95°C, 15 s; 55°C, 15 s; 72°C, 17 s. At the end of each run, melting curves were recorded to ensure the specificity of the reaction products. Amplicons with cycle thresholds >35 were excluded from analysis. Data were analyzed with iQ5 Optical System Software 2.0 (BioRad). A semi-customized PCR-array facilitating the analysis of the mRNA expression of 94 genes related to DNA repair, stress signaling, cell cycle regulation and cell death was used (34) for initial screening (primer sequences see Supplementary Table 2, available at *Carcinogenesis* Online). mRNA expression levels were normalized to the amount of glyceraldehyde 3-phosphate dehydrogenase (GAPDH) and beta-actin mRNA. To calculate drug-induced changes in mRNA levels, relative mRNA expression was related to that of the WT control which was set to 1.0. Only alterations in relative mRNA expression of ≤0.5 and ≥2.0 were considered as different from control. mRNA expression data obtained from the PCR-array-based screening analyses were confirmed by separate quantitative reverse transcriptase polymerase chain

reaction (qRT–PCR) analyses performed in triplicate. Since complementary DNA generated from pooled RNA samples (n = 3–6) was used for q-RT-PCR analyses, statistical analysis was omitted in these experiments.

Preparation of protein extracts and western blot analysis

For preparation of total liver protein extracts, 10–15 mg of liver tissue was homogenized in lysis buffer (Roti®-Load 1) (Carl Roth, Karlsruhe, Germany) using a TissueLyser (Qiagen, HIlden, Germany). Proteins were separated by SDS-PAGE (10–15% polyacrylamide gels) and transferred onto nitrocellulose membranes. After blocking in 5% non-fat milk in TBS/0.1% Tween 20 (60 min, room temperature), membranes were incubated with the primary antibody (1:100–1000; overnight at 4 °C). After washing, incubation with horseradish peroxidase-labeled secondary antibody (1:2000, 2 h, room temperature) was performed. Bound antibodies were visualized using a chemiluminescence imager (Fusion Fx7) (Peqlab, Erlangen, Germany). The following antibodies were used: Rac1, Cyp2E1, *p*-ERK (pThr202/pTyr204), *p*-Foxo1/3a (pThr24;pThr32), p27 (Millipore, Billerica, MA), γH2AX (pS139), GAPDH, heme oxygenase-1 (HO-1), *p*-c-Jun (pS63) (Epitomics, Burlingame, CA), myeloperoxidase (MPO), CD62E (Abcam, Cambridge, UK), S10 phosphorylated histone H3 (*p*-H3) (pS10) (Invitrogen, Paisley, UK), *p*-JNK (pThr183/pTyr185), *p*-Mdm2 (Ser166), ERK2, p16, p21, p38, p53, sTNFα (Santa Cruz, CA), *p*-ATM (S1981), *p*-ATR (S428), Akt, *p*-Akt (pS473), BRCA1, DNA repair protein RAD51 homolog (Rad51), Foxo1, Foxo3a, p53 (pS15), *p*-p38 (pThr180/pTyr182) (New England Biolabs, Frankfurt, Germany), c-Jun-N-terminal kinase (JNK) (Sigma-Aldrich GmbH, Hamburg, Germany). Representative blots were shown. In general, relative protein expression in WT cells was set to 1.0. Densitometrical analysis was done by use of ImageJ. Quantitative data shown below the corresponding representative autoradiographies (-fold differences) are based on the analysis of 2–3 independent samples. According to the information of the supplier (Millipore, Billerica, MA) the Rac1 antibody cross-reacts with Rac2. To verify this, its reactivity was tested against recombinant Rac1, Rac2 and Rac3 protein, which was provided by R. Ahmadian (Institute of Biochemistry and Molecular Biology II, HHU Düsseldorf, Germany). The results obtained show that the Rac1 antibody cross-reacts with recombinant Rac2 and Rac3 (data not shown).

Determination of MGMT activity

The activity of the DNA repair protein O^6-methylguanin-DNA-methyltransferase (MGMT) was determined as described (35).

Immunohistochemistry and immunofluorescence

Paraffin-embedded (formalin-fixed) liver tissue was used for the production of sections of ~4 µm thickness. Paraffin removal, rehydration and demasking of antigens was performed according to standard procedure. Sections were blocked with Protein Block (Dako, Hamburg, Germany) for 120 min and incubated with primary antibody (1:100; 4°C; overnight). As secondary antibodies, horseradish peroxidase-coupled anti-rabbit/mouse (Dako, Hamburg, Germany) and Alexa Fluor 488-coupled anti-goat (Invitrogen, Darmstadt, Germany) antibody were used for immunohistochemistry and immunofluorescence, respectively. To visualize bound antibodies Dako REAL EnVision Detection System (Dako, Hamburg, Germany) was employed. For immunofluorescence analyses, Vectashield (Vector Laboratories INC, Burlingame, CA), which includes the DNA staining dye DAPI, was used. Tissue sections were evaluated microscopically (Olympus BX43). The following antibodies were applied in these studies: E-Cadherin (BD Bioscience, San Jose, CA), *p*-ERK (pThr 202/pTyr 204), ß-catenin (Millipore, Billerica, MA), MPO (Abcam, Cambridge, UK), *p*-H3 (pS10) (Invitrogen, Paisley, UK), glutamine synthase (GS) (Thermo scientific, Waltham, MA), γH2AX (pS139) (Epitomics, Burlingame, CA), p27, cyclinB1 and 53BP1 (New England Biolabs, Frankfurt, Germany).

Analysis of cell death and proliferation

To analyse the frequency of apoptotic liver cells the InSitu Cell Death Detection Kit (Roche Diagnostics, Mannheim, Germany) was used. The frequency of mitotic cells was determined by calculating the percentage of phospho-histone H3 (pS10) positive cells. Three to five liver sections were scored per animal.

Analysis of DNA damage

Ser139 phosphorylated H2AX (γH2AX) is a well accepted surrogate marker of DNA damage, in particular of DNA double-strand breaks (DSBs) (36). The level of S139 phosphorylated histone H2AX (γH2AX) was determined by western blot analysis. Moreover the number of γH2AX positive nuclei in liver sections was captured by immunohistochemistry.

Statistical analyses

Statistical analyses was performed by use of the Student's *t*-test.

Results and discussion

Lack of Rac1 reduces DEN-induced formation of liver tumors

In order to generate mice that are characterized by a conditional KO of the *rac1* gene in the liver, $Rac1^{flox/flox}$ mice (8) were bred with mice expressing the Cre-recombinase under control of the hepatocyte specific Alb promotor. This promotor is reported to trigger Cre expression in fetal and neonatal mice with maximum Cre levels reached 7 days after birth (30). In order to address the question whether Rac1 signaling influences the formation of liver tumors, mice 2 weeks of age were treated with a single dose of DEN (10 mg/kg, i.p.), which is frequently used for chemical induction of liver tumors (31,37), and the tumor burden in the liver was analyzed after post-incubation period of 40 weeks. Since some reports showed only a partial recombination of floxed alleles with Alb-Cre during early development, while other studies reported on a significant Alb-Cre function already in fetal and neonatal mice (29,30), we determined the extent of *rac1* gene deletion in our mouse model. As shown on the level of the DNA and the protein, the Alb-Cre driven deletion of the *rac1* gene was already highly efficient (i.e. ~80–90%) in the two week old mice (Figure 1A) and comparable to what we observed in elder (i.e. 10–12 week old) mice (Supplementary Figure S1, available at *Carcinogenesis* Online). Because the Alb-Cre promotor is specific for hepatocytes, we assume that the residual 10–20% of Rac1 expression in $Rac^{flox/flox/Alb\text{-}Cre}$ mice mainly originates from other cell types of the liver. Since the Rac1 antibody also detects recombinant Rac2 and Rac3 protein, it appears likely that this cross-reactivity of the Rac1 antibody with other Rac isoforms (i.e. Rac2 and Rac3) (data not shown) also contributes to the signal. As opposed to WT animals, no tumors could be macroscopically detected in *rac1* KO mice (Figure 1B). Microscopic analyses of liver sections, however, showed the presence of a low number of small-sized tumors also in *rac1* KO animals (Figure 1C). Hence, incidence and average size of liver tumors induced by DEN are largely reduced in the absence of *rac1*. Correspondingly, Rac1 regulates mechanisms that facilitate the formation of mouse liver tumors following DEN exposure. To rule out the possibility that the tumors formed in $Rac1^{flox/flox/Alb\text{-}Cre}$ animals result from hepatocytes that have escaped from Cre-mediated deletion of *rac1*, the expression of Rac1 protein was analyzed in the corresponding tumors. Since none of the small-sized tumors formed in $Rac1^{flox/flox/Alb\text{-}Cre}$ animals expressed Rac1 protein (Figure 1D), this possibility can be excluded. Notably, about 20% of the tumors grown in Rac1 proficient mice featured overexpression of Rac1 in tumor tissue as compared to the surrounding normal tissue (Figure 1D). This finding is in line with reports showing overexpression of Rac1 protein in different types of human tumors (38,39).

More detailed molecular characterization of the tumors formed in the presence or absence of Rac1 revealed *p*-ERK

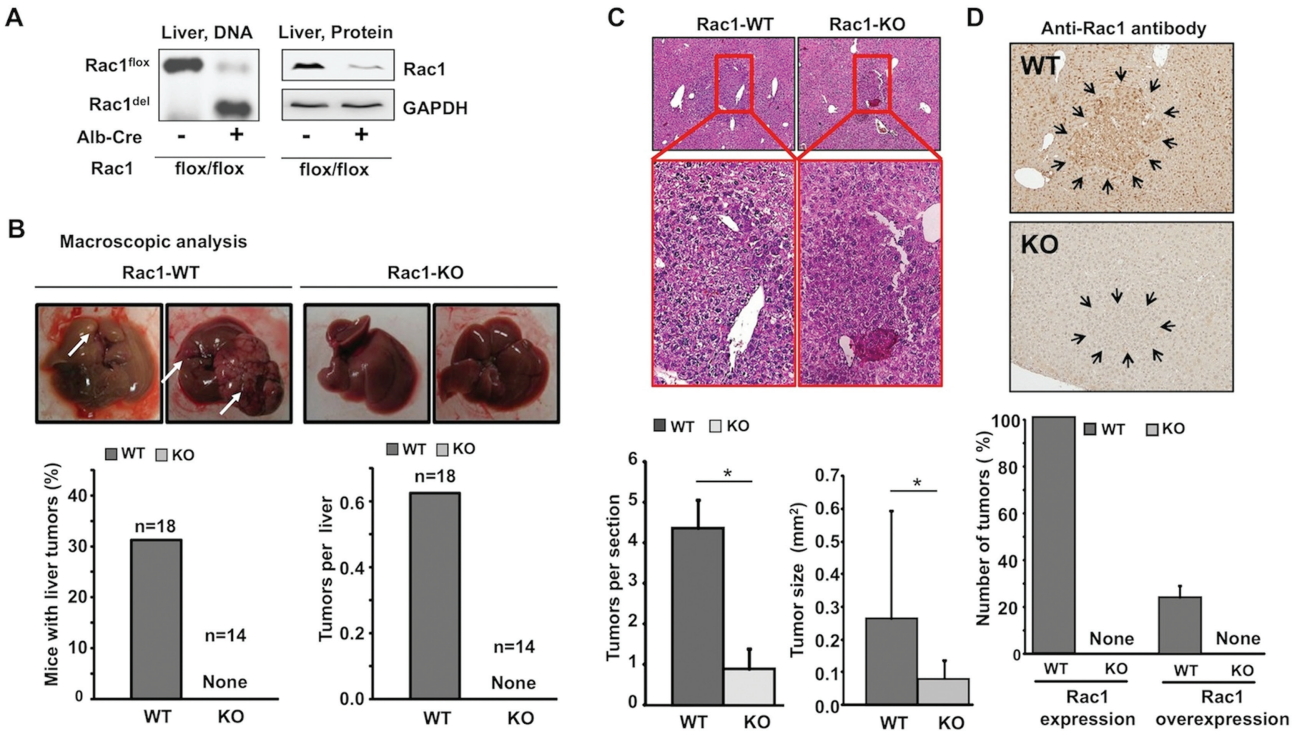

Figure 1. Rac1 KO protects against DEN-induced formation of liver tumors. (**A**) The efficiency of the liver specific *rac1* KO in $Rac^{flox/flox/Alb\text{-}Cre}$ mice, which were generated by breeding of $Rac^{flox/flox}$ with Alb-Cre expressing mice, was analyzed in animals 2 weeks of age on the level of the DNA by genomic PCR and on the level of the protein by western blot analysis. Expression of GAPDH protein was determined as a loading control. (**B**) Liver of WT (Rac1-WT) and *rac1* KO mice was examined macroscopically for the formation of tumors 40 weeks after single treatment of young mice (i.e. 2 weeks of age) with DEN (10 mg/kg; i.p.). Representative pictures of each two livers from WT or KO mice are shown. Arrows point to single tumors. Quantitative data shown are the mean number of tumors (in percent) detected in WT ($n = 18$) and *rac1* KO ($n = 14$) mice (left panel) and the average number of tumors per liver (right panel). (**C**) Microscopic analysis of tumor formation was performed in H&E stained liver sections of DEN-treated WT (Rac1-WT) and *rac1* KO mice. Boxes show tumor areas of WT and KO mice in higher magnification (i.e. ×20). Quantitative data showing the number of tumors per section are the mean ± SD from $n = 14$–18 animals with each three liver sections analyzed per mouse. For quantitative analysis of the tumor size (mean ± SD), H&E stained liver sections from Rac1 proficient (WT) and Rac1 deficient mice (KO) containing tumorigenic areas were analyzed. Data are the mean ± SD obtained from the analysis of $n = 14$–18 mice per group. *$P \leq 0.05$. (**D**) Liver sections from Rac1 proficient $Rac1^{flox/flox}$ (WT) and Rac1 deficient $Rac1^{flox/flox/Alb\text{-}Cre}$ mice (KO) containing tumorigenic areas were stained with Rac1-specific antibody. For quantitative analysis (mean ± SD), livers from $n = 6$ mice per group with each 2–10 tumors per mouse have been analyzed. None of the tumor areas found in $Rac1^{flox/flox/Alb\text{-}Cre}$ mice expressed Rac1. About 20% of the tumor areas of Rac1 proficient $Rac1^{flox/flox}$ mice showed overexpression of Rac1 protein as compared to the surrounding normal tissue.

positive tumors in WT mice (Figure 2A), which is in line with previous reports (32,40). By contrast, all tumors formed in *rac1* KO animals were *p*-ERK negative (Figure 2A). This indicates that DEN-initiated hepatocarcinogenesis in the absence of Rac1 is independent of the Ras/Raf pathway. If present, Rac1 facilitates Ras-mediated hepatocarcinogenesis. This is in line with previous report showing that Rac1 is required for the formation of lung tumors induced by oncogenic K-Ras (24). Therefore, we suggest that Rac1 acts in concert with Ras, thereby fostering tumor formation *in vivo*. Moreover, most of the tumors observed in the liver of both WT and *rac1* KO mice were negative for the expression of GS (Figure 2B), which is a marker of activating mutations in the ß-catenin pathway (41). ß-catenin is a key player in Wnt-driven hepatocarcinogenesis (32). It is controlled by Rac1-dependent pathway in colon cancer cells (42,43). In line with the GS data, we found no obvious difference between the expression levels of ß-catenin in liver tumors of Rac1-proficient and -deficient mice (Figure 2C). A small subset of cells found in tumors of WT animals were GS positive (Figure 2B). This phenomenon of a nonhomogenous GS-staining of tumors was not observed in the small-sized liver tumors found in *rac1* KO mice. It appears conceivable that this phenomenon is related to the fact that Rac1 is required for nuclear transport of ß-catenin (44). Accordingly, we observed a lower level of ß-catenin in the nuclei of Rac1-deficient hepatocytes as compared to Rac1-proficient liver cells (Supplementary Figure S2, available at *Carcinogenesis* Online). In conclusion, DEN-stimulated tumor formation in the absence of Rac1 likely does not require translocation of ß-catenin into the nucleus. We would like to note that ß-catenin is of particular relevance for phenobarbital-mediated promotion of liver tumor formation (32,37). Whether Rac1 impacts tumor promotion by phenobarbital will therefore be subject of forthcoming studies.

Moreover, we also monitored the expression of the cell adhesion molecule E-cadherin, which is involved in the regulation of Wnt signaling (45,46) and, most important, is regulated in a Rac1-dependent manner (47–49). The data show a sharp separation of the tumor area from the normal tissue in WT animals, which was not the case when Rac1 protein is missing (Figure 2D). The frequency of cells showing cytosolic expression of E-cadherin was increased in *rac1* KO animals as compared to WT animals, indicating that E-cadherin-regulated cell-cell interaction of tumor cells is disturbed under situation of Rac1 deficiency. Consistent with this finding, Rac1 is reported to prevent endocytosis of E-cadherin (49). The finding of a lower frequency and size of liver tumors in *rac1* KO mice could depend on a reduced proliferation rate or a higher frequency of apoptosis.

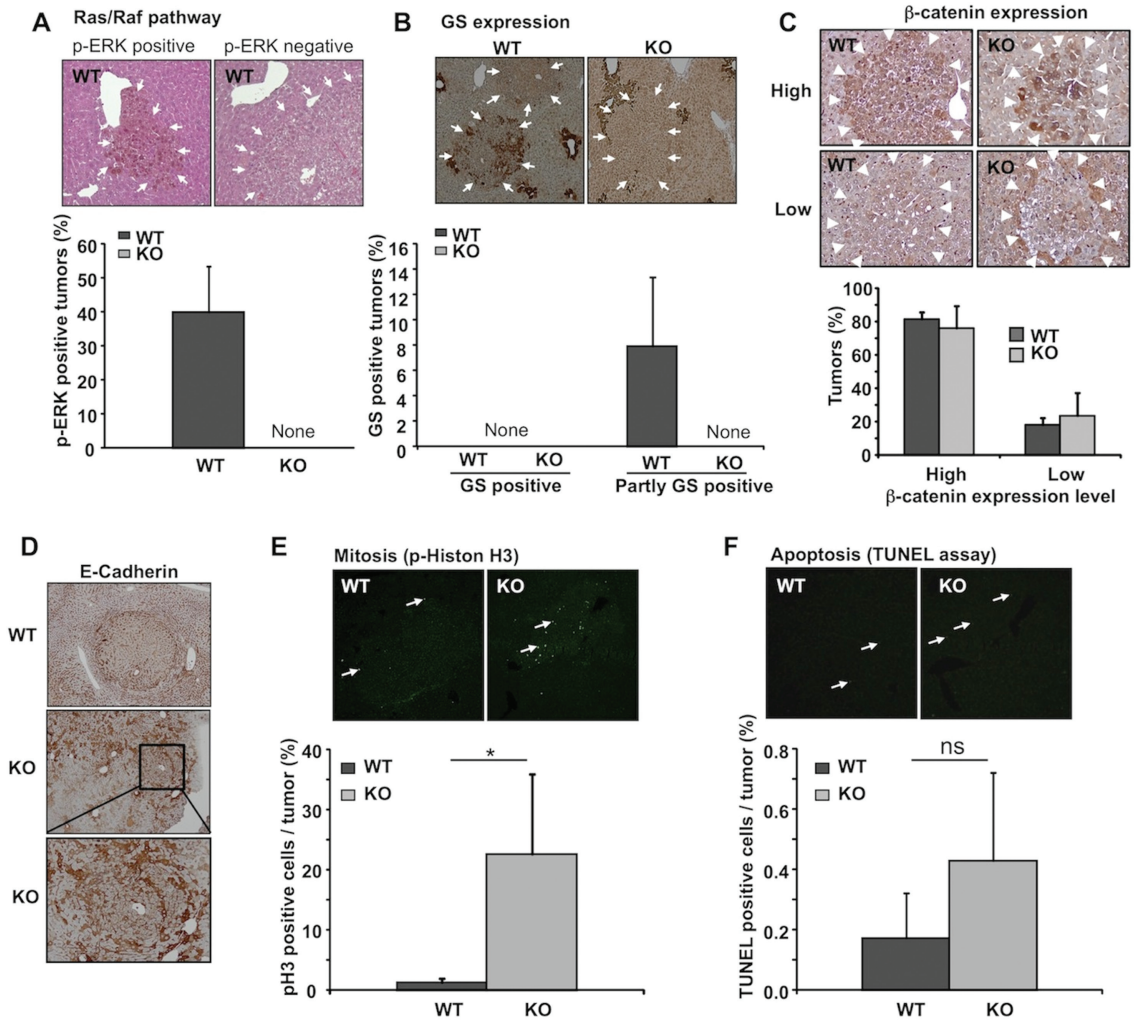

Figure 2. Liver tumors that are induced by DEN in the absence of Rac1 are *p*-ERK and GS negative and show an increased number of *p*-H3 positive cells. (A–D) DEN-induced tumors of WT and *rac1* KO mice were analyzed for the expression of *p*-ERK (**A**), GS (**B**), beta-catenin (**C**) and E-cadherin (**D**). Arrows shown in (A–C) mark the edges of the tumor areas. Quantitative data (mean ± SD) are based on the analysis of the liver from $n = 6$ animals per group with each 2–10 tumors being analyzed per mouse. (**E**) Liver sections from WT mice and mice lacking hepatic Rac1 expression (KO) that contain tumorigenic areas were stained with *p*-histone H3 specific antibody (arrows point to *p*-H3 positive cells). For quantitative analysis (mean ± SD), livers from $n = 6$ mice per group with each 2–10 tumors per mouse have been analyzed. *$P \leq 0.05$. (**F**) The frequency of TUNEL positive cells in liver sections of WT mice and mice lacking hepatic Rac1 expression (KO) was determined as described in methods. The ratio between TUNEL positive tumor cells and the number of total tumor cells per area was calculated and shown in percent. Arrows exemplarily point to TUNEL positive cells. For quantitative analysis (mean ± SD), livers from $n = 6$ mice per group with each 2–10 tumors per mouse have been analyzed. ns = statistically not significant.

The frequency of *p*-H3 positive (i.e. G2/M) cells was significantly higher in liver tumors of *rac1* KO animals as compared to tumors of WT mice (Figure 2E). Also, tumors from *rac1* deficient mice showed stronger nuclear expression of cyclin B1 while nuclear expression of p27 was similar to the WT (Supplementary Figure S3, available at *Carcinogenesis* Online). Spontaneous apoptosis, which was analyzed by the Terminal Deoxynucleotidyl Transferase-Mediated dUTP Nick End Labeling (TUNEL) assay, was slightly (but statistically not significant) enhanced in the absence of Rac1 (Figure 2F). Taken together, we conclude that the reduced size of tumors grown in the absence of Rac1 reflects a mitotic arrest of tumor cells rather than increased frequency of apoptosis. It is conceivable that Rac1 is required for mitotic progression of DEN-initiated malignant cells *in vivo*. This hypothesis is supported by recent *in vitro* findings showing that Rac1 is essential for the regulation of mitosis (4,50). Taken together, the data indicate that Rac1 is required for the clonal outgrowth of initiated cells.

Rac1 impacts basal and DEN-induced expression of metabolic liver enzymes

In order to study the influence of Rac1 on mechanisms related to tumor initiation, early hepatic stress responses provoked by DEN were analyzed. To ensure substantial activation of hepatic stress responses, WT and *rac1* KO animals were treated with a single high dose of the alkylating liver-specific carcinogen diethylnitrosamine (DEN) (90 mg/kg; i.p.). The Alb-Cre driven hepatic KO efficacy of *rac1* in these animals (10–12 weeks of age) was ~80–90% as shown on the level of the gene, the mRNA and the protein (Supplementary Figure S1, available at *Carcinogenesis* Online). This is similar to what we observed in the young (2-week old) mice (Figure 1A). After posttreatment period of 24 h and 72 h, alterations in mRNA and protein expression levels were analyzed by qRT–PCR and western blot analysis, respectively. As metabolic activation of DEN is mainly achieved by cytochrome P450 type 2E1 (Cyp2E1), its basal mRNA expression was investigated. The data show that basal Cyp2E1 mRNA expression was reduced by

about 60% in the absence of Rac1 (Figure 3A). Decrease in basal Cyp2E1 mRNA level in *rac1* KO mice was reflected on the protein level (Figure 3C). The mRNA expression of Cyp1A1 and Cyp1B1, which were included for control, showed about 40% reduction in the level of Cyp1A1 mRNA, while the level of Cyp1B1 mRNA remained largely unaffected (Figure 3A). The mRNA level of the damage defense factor glutathione-S-transferase M1 (Gstm1) was slightly enhanced in the absence of Rac1, the expression of heme oxygenase-1 was reduced by ~50% (Figure 3A). As analyzed 24 h after DEN treatment, the *rac1* status had no major influence on the mRNA levels of cytochrome P450s or detoxifying proteins (Figure 3B). Yet, when investigated 72 h after DEN treatment, the mRNA levels of Cyp1A1 and Cyp1B1 increased by 4–5 fold in *rac1* KO animals, whereas WT mice showed a much weaker response (Figure 3B). The protein level of Cyp2E1 was similar in WT and *rac1* KO mice 24 h after DEN treatment and likewise decreased 72 h after DEN exposure independent of the *rac1* status (Figure 3C). Regarding heme oxygenase-1 mRNA, WT animals showed a stronger induction 72 h after DEN exposure as compared to *rac1* KO mice (Figure 3B). In line with this, increased expression of heme oxygenase-1 protein was also found 72 h after DEN treatment of WT mice as compared to DEN treated Rac1 deficient mice (Figure 3C). Taken together, the data show that Rac1 has multiple effects on both basal and DEN-stimulated expression of factors that are involved in the activation or detoxification of chemical carcinogens. Apparently, Rac1 regulates liver functions involved in the metabolism of xenobiotics.

Hepatic rac1 KO results in enhanced DDR as well as reduced expression of DNA repair factors following exposure to DEN

DNA damage plays a pivotal role in tumor initiation. To investigate the influence of Rac1 on the formation of DNA damage and the DDR, activation of ATM/ATR kinases, which are the key regulators of the DDR (51), was monitored 24 h and 72 h after DEN exposure. Under our experimental conditions, no increase in the level of S1981-phosphorylated ATM (*p*-ATM) was observed (Figure 4A). However, DEN treatment caused a substantial increase in the protein level of S428-phosphorylated ATR, both 24 h and 72 h after exposure (Figure 4A). A stronger activation of ATR following DEN treatment was observed in the absence of Rac1 protein (Figure 4A). Next, we analyzed S139 phosphorylation of histone H2AX (γH2AX), which is a generally accepted surrogate marker of DNA damage, in particular DSBs (36,52,53). As shown by western blot analysis, Rac1 deficiency resulted in an increased level of γH2XA protein when analyzed 24 h and 72 h after DEN treatment (Figure 4A). Counting the number of γH2AX positive cells by immunohistochemistry, identical effects were observed (Figure 4B). These studies disclosed a mixture of γH2AX pan-stained cells and cells containing distinct γH2AX foci (Figure 4B and Supplementary Figure S3, available at *Carcinogenesis* Online). This indicates that DEN treatment caused stalled replication forks, which trigger H2AX phosphorylation in an ATR dependent manner (54), as well as DSBs. The formation of DSBs following DEN treatment was confirmed by the analysis of 53BP1

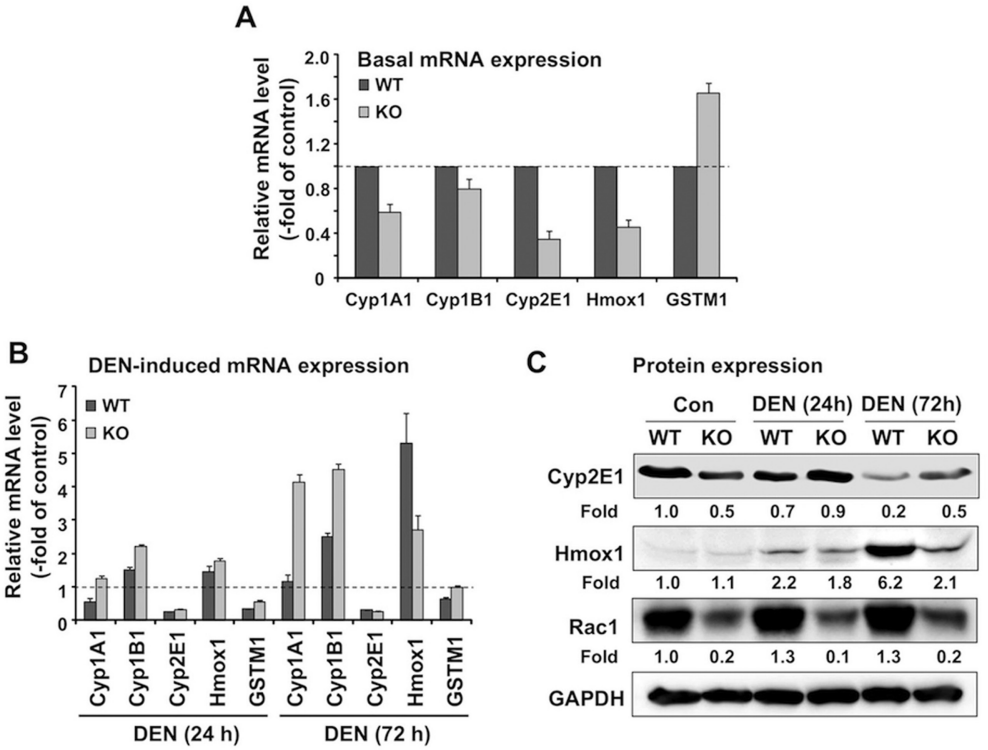

Figure 3. Effect of *rac1* KO on basal and DEN-induced expression of factors involved in drug metabolism. (**A** and **B**) The influence of hepatic *rac1* KO on the mRNA expression of a selected subset of factors involved in drug metabolism and detoxification was analyzed by quantitative RT-PCR. Basal mRNA expression was investigated in untreated WT and *rac1* deficient mice (KO) (A) as well as 24 h and 72 h after treatment of WT and KO mice (10–12 weeks of age) with a single dose of DEN (90 mg/kg; i.p.) (B). mRNA expression levels were normalized to the corresponding untreated WT control which was set to 1.0 (dashed line). qRT–PCR was done in triplicate as described in methods. The extent of *rac1* gene deletion in 10–12 week old mice is shown in Supplementary Figure S1, available at *Carcinogenesis* Online. (**C**) Protein expression was analyzed in total liver extracts of WT and *rac1* KO mice that were left untreated (Con) or were treated with DEN (90 mg/kg; i.p.) as described in methods. 24 h and 72 h after injection of DEN, protein expression was analyzed by western blot analysis using the indicated antibodies. Protein expression of GADPH was monitored as loading control. Relative expression in the untreated WT was set to 1.0. Shown are representative autoradiographies from two independent experiments. Quantitative data are based on densitometrical analyses as described in methods.

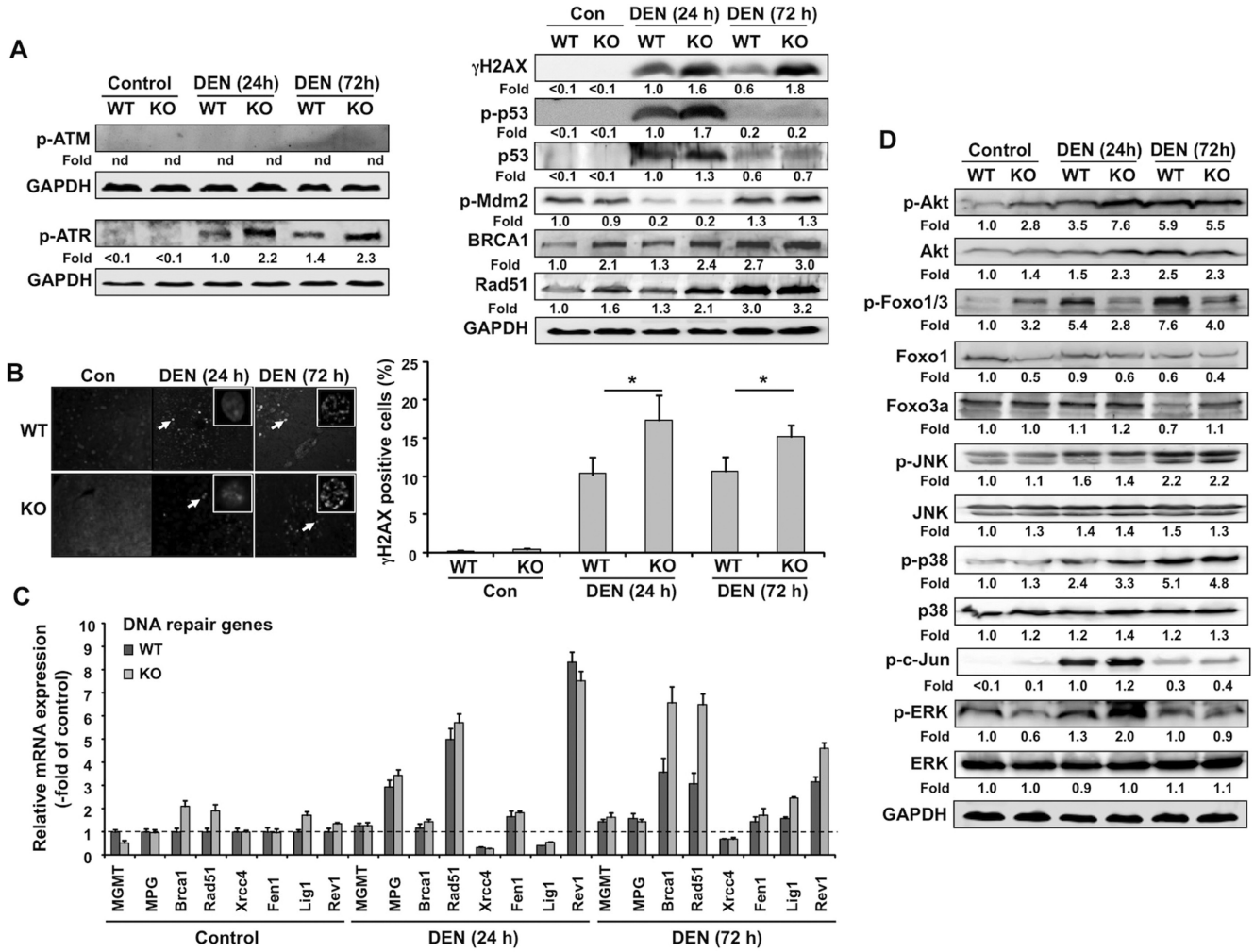

Figure 4. Lack of Rac1 protein promotes acute DEN-induced DDR and stimulates the expression of a subset of DNA repair genes. (**A**) Protein expression of factors reflecting the activation of the DDR (*p*-ATM, *p*-ATR, γH2AX, *p*-p53) and factors involved in the repair of DSBs by homologous recombination (Brca1, Rad51) was analyzed by western blot analysis. Total liver extracts from untreated (Con) or DEN treated WT and *rac1* KO mice were isolated 24 h and 72 h after DEN treatment (90 mg/kg; i.p.). Protein expression of GADPH was monitored as loading control. Relative expression in the WT was set to 1.0. Shown are representative autoradiographies from two independent experiments. nd = not detectable. Quantitative data are based on densitometrical analyses as described in methods. (**B**) The frequency of γH2AX positive nuclei was determined in liver sections of WT and Rac1 deficient (KO) mice 24 h and 72 h after DEN (90 mg/kg; i.p.) treatment. Stained nuclei were counted and related to the total number of nuclei. Arrows exemplarily point to γH2AX positive nuclei. Inserts represent single γH2AX positive nuclei in higher magnification, showing that DEN treatment results in both pan-staining and formation of distinct foci. Quantitative data shown are the mean ± SD from $n = 3$–4 animals. At least three liver sections per animal were subjected to analysis. *$P \leq 0.05$. See also Supplementary Figure S4, available at *Carcinogenesis* Online. (**C**) To investigate the basal (Control) and DEN-induced mRNA expression levels of a subset of DNA repair genes, mRNA was isolated from liver 24 h and 72 h after DEN treatment (90 mg/kg; i.p.). Quantitative analysis of mRNA levels was performed by qRT–PCR (triplicate determinations) as described in methods. Relative mRNA expression in untreated WT was set to 1.0 (dashed line). (**D**) Total liver extracts that were isolated from untreated (Control) animals or 24 h and 72 h after DEN treatment (90 mg/kg; i.p.) of WT and *rac1* KO mice were analyzed with respect to the activity status of a subset of protein kinases and related transcription factors by western blot analysis using the indicated phospho-specific antibodies (see materials for phosphorylated residues). For protein loading control, the membrane was reprobed with anti-GAPDH specific antibody. Relative expression in the untreated WT was set to 1.0. Autoradiographies show a representative result of two independent experiments ($n = 3$ mice). Quantitative data are based on densitometrical analyses as described in methods.

foci formation, again showing a higher frequency of 53BP1 positive cells in the absence of Rac1, and partial co-localization of γH2AX and 53BP1 foci (Supplementary Figure S4, available at *Carcinogenesis* Online). As analyzed 24 h after DEN treatment, Rac1 deficiency also augmented the level of S15 phosphorylated p53 protein (*p*-p53) as compared to the WT (Figure 4A). S15 phosphorylation of p53 is a mechanism of p53 stabilization by ATM after DNA damage (55). *p*-p53 levels normalized 72 h after DEN exposure in both WT and *rac1* KO animals (Figure 4A). Protein level of *p*-Mdm2 transiently decreased 24 h after DEN treatment independent of the *rac1* status (Figure 4A). Bearing in mind that Rac1 regulates the activity of the transcription factor AP-1 (13), which gets activated by various genotoxins and regulates of the expression of multiple DNA repair genes (56), we next analyzed the expression of factors that are involved in the processing of DNA double-strand breaks. The expression of Brca1 and Rad51, which are involved in the repair of DNA double-strand breaks by homologous recombination (57), was enhanced in *rac1* KO mice (Figure 4A). As shown in Figure 4C, basal mRNA expression of the repair gene MGMT, which plays a key role in the repair of DNA methylation damage (58), was only minorly affected if *rac1* is absent. In line with this, hepatic MGMT activity was similar in the presence or absence of Rac1 (99.3 ± 9.9 fmol/mg protein ($n = 6$) in WT and 98.3 ± 13.9 fmol/mg protein ($n = 6$) in *rac1* KO animals). This indicates that O^6-methylguanine induced

by DEN and its repair by MGMT does likely not account for the observed differences in the DDR (Figure 4A). In line with the western blot-based data (Figure 2A), basal mRNA expression of Brca1 and Rad51 was enhanced by about 2-fold in the absence of the *rac1* gene (Figure 4C). Since the Rac1 deficient $Rac1^{flox/flox/Abl\text{-}Cre}$ mice express the Cre-recombinase, which may cause unspecific DNA damage thereby triggering DNA damage responses, we investigated the expression of Brca1 and Rad51 in Alb-Cre mice harbouring WT Rac1 protein ($Rac1^{wt/wt/Alb\text{-}Cre}$). These analyses showed that basal mRNA and protein expression of Brca1 and Rad51 are specifically upregulated in Rac1 deficient $Rac1^{flox/flox/Abl\text{-}Cre}$ mice but not in Cre expressing mice harbouring WT Rac1 (Supplementary Figure S5, available at *Carcinogenesis* Online). Correspondingly, upregulation of the aforementioned DSB repair factors is the consequence of Rac1 deficiency rather than the expression of Cre recombinase. The observation that Rac1 deficient hepatocytes do not show elevated basal protein levels of γH2AX or *p*-p53 (Figure 4) further argues against a significant formation of DNA damage by the expression of Cre protein.

Analysis of gene expression 24–72 h after DEN treatment revealed an increase in the mRNA levels of N-methylpurine-DNA-glycosylase (MPG), Rad51 and Rev1, which was independent of *rac1* status (Figure 4C). By contrast, 72 h after DEN treatment, the mRNA levels of Brca1 and Rad51 were higher if *rac1* is deleted (Figure 4C). Taken together, the mRNA and protein data provide novel *in vivo* evidence that Rac1 signaling represses the expression of DSB-associated DNA repair genes and, moreover, attenuates the DNA damage response. Bearing in mind that *rac1* KO caused a decrease in the basal mRNA expression of Cyp2E1, which is involved in metabolic activation of DEN (59), a reduced level of DNA damage and, correspondingly, an attenuated DDR may have been anticipated in *rac1* KO animals. However, the opposite was observed: lack of Rac1 enhanced the DDR following DEN treatment. Hence, the data point to an inhibitory function of Rac1 in the DDR stimulated by DEN. In a previous study we have observed that Rac1 is required for activating the DDR in hepatocytes when exposed to the anthracycline derivative doxorubicin (60), which induces DNA

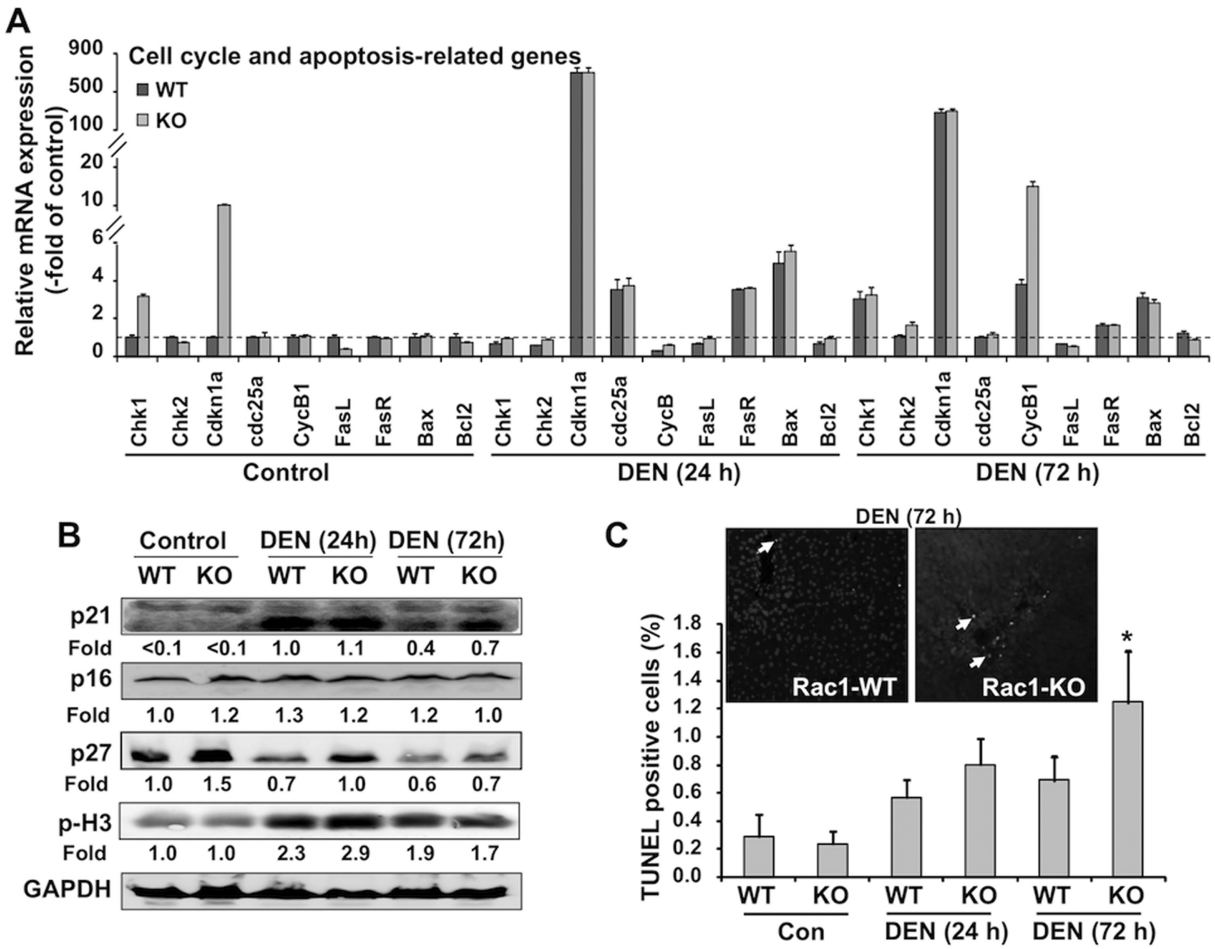

Figure 5. *rac1* KO impacts the expression of cell cycle regulatory factors and promotes induction of cell death. (**A**) The hepatic mRNA expression of cell cycle and apoptosis-related genes was analyzed 24 h and 72 h after DEN treatment (90 mg/kg; i.p.) of WT and *rac1* KO mice by qRT–PCR as described in methods. Data shown are from triplicate determinations. Relative mRNA expression in untreated control was set to 1.0 (dashed line). (**B**) Total liver extracts were isolated from untreated (Control) animals or 24 h and 72 h after DEN treatment of WT and *rac1* KO mice. The expression level of a subset of CDK inhibitors (p16, p21, p27) was analyzed by western blot using the indicated antibodies. In addition, Ser10 phosphorylation of histone H3 (*p*-H3), which is indicative of chromosome condensation in G2/M phase cells, was analyzed by use of phospho-specific antibody. For protein loading control, the membrane was reprobed with anti-GAPDH specific antibody. Relative expression in the WT was set to 1.0. Shown are representative autoradiographies from two independent experiments. Quantitative data are based on densitometrical analyses as described in methods. (**C**) In order to analyze the frequency of apoptotic cells the TUNEL assay was used. Mice were treated with DEN as described under A. Arrows indicate TUNEL positive cells. Quantitative data shown are the mean ± SD from n = 3–4 animals per group with ≥3 liver sections being analyzed per animal. *$P \leq 0.05$ [as compared to DEN (72 h) treated WT mice].

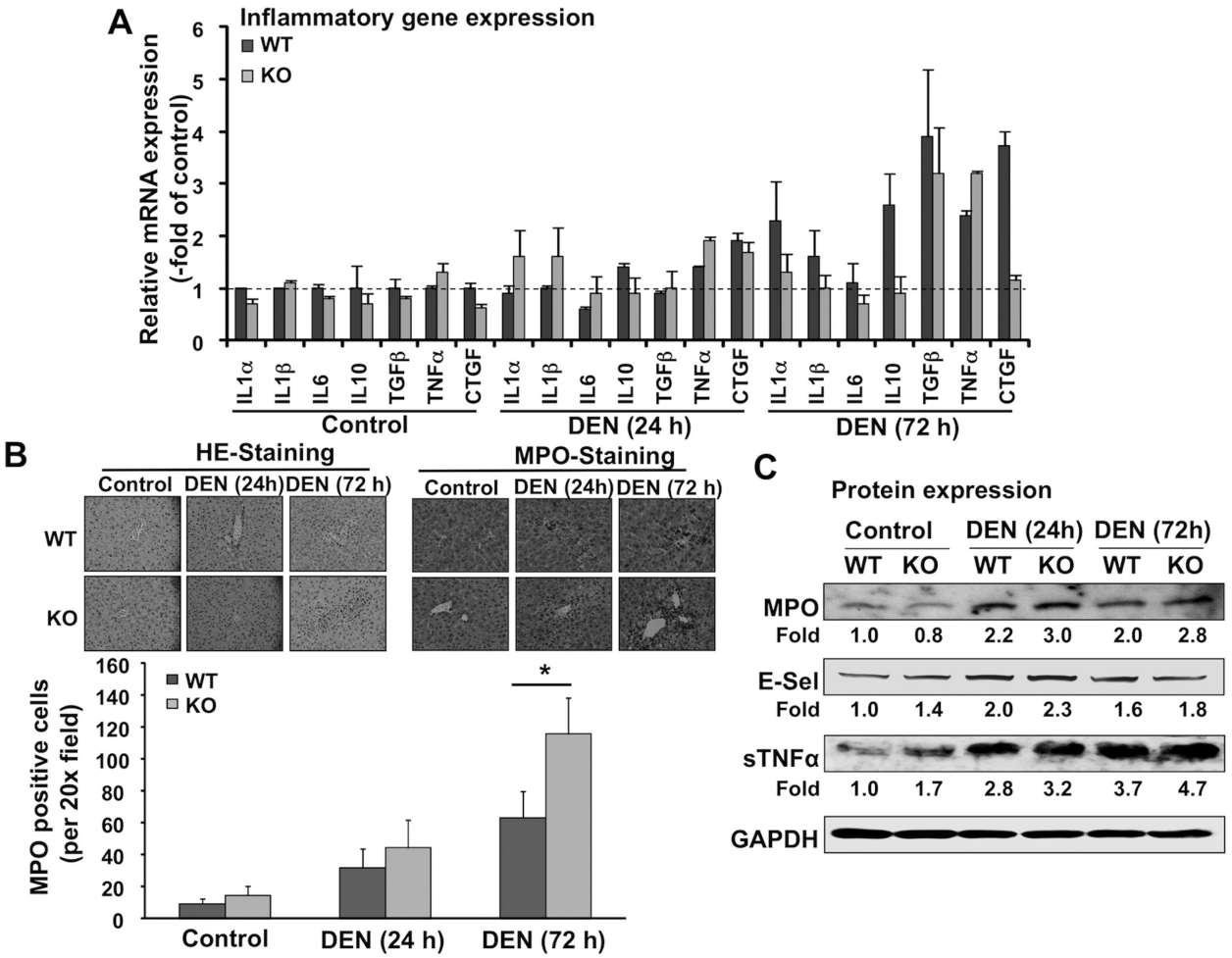

Figure 6. Rac1 deficiency influences the mRNA expression of cytokines that are related to inflammation and fibrosis. (**A**) Basal and DEN-induced changes in the mRNA expression of inflammatory genes was analyzed in the liver of untreated mice (Control) or 24 h and 72 h after DEN treatment (90 mg/kg; i.p.) of *rac1* WT and *rac1* KO animals by qRT–PCR (triplicate determinations). Relative expression in untreated WT was set to 1.0. (**B**) Infiltration of liver tissue by immune cells was analyzed by H&E staining and by counting the number of MPO expressing cells. Quantitative data represent the number (mean ± SD) of MPO positive cells detected by microscopic analysis (per 20× field) of liver sections from $n = 4$ animals with ≥3 liver sections per animal being investigated. *$P \leq 0.05$. (**C**) Protein expression of the indicated factors was analyzed in total liver extracts from untreated (Control) or DEN treated WT and Rac1 deficient (KO) mice by western blot analysis. Relative protein expression in the WT was set to 1.0. Autoradiographies are representative of two independent experiments. Quantitative data are based on densitometrical analyses as described in methods.

damage by inhibition of topoisomerase II isoforms. Therefore, we assume that the biological relevance of Rac1 for the regulation of the DDR depends on the type of the genotoxin.

Depending on the cellular context, Rac signaling has either a pro-survival or pro-apoptotic role *in vitro* (61,62). Since apoptosis works against tumor formation, we next investigated the influence of Rac1 deficiency on a selected subset of stress-inducible signaling pathways and transcription factors that are known to be regulated in a Rac1-dependent manner and/or affect pathways of cell survival and death. These analyses show that basal *p*-Akt level was higher in *rac1* KO animals than in the corresponding WT (Figure 4D). This result was unexpected since Rac1 is reported to activate Akt (63). Basal phosphorylation of the transcription factor Foxo1/3, which is a major target of Akt signaling (64) and is involved in the regulation of p27 (65) and Cyp2E1 expression (66), was also enhanced in the absence of *rac1* (Figure 4D). Yet, whereas the *p*-Foxo1/3 level largely increased in WT animals treated with DEN, this response was no longer observed if *rac1* was missing (Figure 4D). Obviously, Rac1 signaling is essential for DEN-stimulated phosphorylation of the transcription factor Foxo1/3. As the level of *p*-Akt did not parallel the level of *p*-Foxo1/3 (Figure 4D), we suppose that the DEN-stimulated increase in the phosphorylation of Foxo 1/3 is independent of Akt kinase. As it is known that Foxo proteins can directly interact with ATM (67), we speculate that the augmented DDR in *rac1* KO mice promotes ATM/Foxo interaction, which in turn results in a reduced accessibility of Foxo 1/3 for phosphorylation by Akt. Considering that Rac1 is known as a major regulator of mitogen-activated protein kinase and downstream AP-1-like transcription factors (11,12), we further investigated their activation status under basal situation and following DEN treatment. Basal and DEN-stimulated phosphorylation of c-Jun-N-terminal kinase (JNK), which is the major c-Jun phosphorylating kinase, and of p38 kinase were not affected by *rac1* deletion (Figure 4D). As compared to the WT, the level of *p*-ERK was enhanced in the absence of *rac1* as observed 24 h after DEN exposure (Figure 4D). A possible explanation for this unexpected finding is that the extracellular regulated kinase (ERK) phosphorylating kinase MEK1/2 is not exclusively regulated in a Rac1 dependent manner. Hence, compensatory mechanisms

resulting from Rac1 deficiency could account for this phenomenon. Taken together, in the liver, Rac1 selectively interferes with MEK1/2-regulated ERK signaling but not with DEN-stimulated and MKK-regulated activation of JNK and p38 kinase. The phosphorylation status of the transcription factor c-Jun, which is reported to control the initiation of liver cancer (68), transiently increased 24 h after DEN treatment. This response was not affected upon *rac1* deletion (Figure 4D).

Rac1 influences the DEN-induced mRNA expression of cell cycle- and cell death-related factors

Regarding the mRNA expression of factors regulating cell cycle progression and death, we found that Rac1 deficiency caused a large increase in the basal mRNA expression of checkpoint kinase 1 (Chk1), but not of Chk2, and of cyclin-dependent kinase inhibitor 1A (p21) (Figure 5A). The mRNA expression of membrane- and mitochondria-associated death-regulatory factors such as Fas-R/Fas-L and Bax/Bcl2, respectively, remained unaffected if the hepatic *rac1* gene was knocked-out. DEN treatment resulted in a >100-fold increase in p21 mRNA level in WT and *rac1* KO mice, both 24 h and 72 h after treatment (Figure 5A). Based on these results and taking into consideration that Rac1 is essential for cell cycle progression and mitosis (69), we analyzed the protein expression of various inhibitors of cyclin-dependent protein kinases, including p21, on the protein level. As shown in Figure 5B, Rac1 had only minor effects on basal p21 protein expression. This finding contrasts with the RNA data (Figure 5A) and may depend on mechanisms of translational control. Following DEN treatment, the p21 protein level was largely increased, which was independent of the *rac1* status (Figure 5B). By contrast, expression of p27 protein was elevated in the absence of *rac1*, both under basal conditions and after DEN exposure, while p16 expression again remained unaffected by the *rac1* status (Figure 5B). Apart from p21 mRNA expression, the mRNA level of the G2/M specific cyclinB1 was also increased in *rac1* KO as compared to WT mice 72 h after DEN administration (Figure 5A). The phosphorylation status of histone H3 (*p*-H3) at Ser10, which is a hallmark of G2/M phase cells (70), was largely stimulated by DEN exposure and was not influenced by Rac1 (Figure 5B). Measuring the frequency of apoptotic cells using the TUNEL assay, we observed a moderate, but statistically significant higher frequency of dead cells in the absence of Rac1 as compared to the WT 72 h after DEN treatment (Figure 5C). This is in line with the finding that Rac1 signaling suppresses apoptosis (71). Since apoptotic cells are quickly removed *in vivo* by the immune system, it might be that the frequency of apoptotic cells is underestimated. We hypothesize that the increase in DEN-induced apoptosis in Rac1 deficient mice results in a more efficient (early) elimination of initiated cells and that this contributes to the lower incidence of liver tumors observed at late time points. The data provide evidence that Rac1 influences the expression of a subset of cell cycle regulatory factors, which is in line with *in vitro* data showing that Rac1-regulated mechanisms are required for cell cycle progression through G1 (72,73) and G2/M (69). Moreover, our data show that Rac1 signaling protects liver cells from the pro-apoptotic effects of DEN treatment. The data are in line with earlier *in vitro* reports showing that Rac1 protects against detachment-induced apoptosis (anoikis) (74).

Effect of hepatic *rac1* KO on acute inflammatory stress responses

Cell death following genotoxin exposure can result in inflammatory stress responses. Therefore, we next investigated the influence of *rac1* KO on the basal and DEN-induced mRNA expression of factors involved in inflammatory processes and tissue remodeling. As shown in Figure 6A pro-inflammatory and -fibrotic stress responses were observed not before 72 h after DEN exposure. The nitrosamine caused an up to 4-fold increase in the mRNA expression of the inflammatory cytokines IL-1α, TNFα and IL-10α as well as of the pro-fibrotic cytokines TGFβ and connective tissue growth factor (Figure 6A). In *rac1* KO mice, the mRNA expression of IL-10α and connective tissue growth factor was largely reduced (Figure 6A). Hematoxylin and eosin (H&E) staining of liver sections obtained 72 h after DEN treatment revealed an increased number of cells with small nuclei around the vessels in *rac1* KO mice, which could be indicative of infiltrating leukocytes. Indeed, visualization of granulocytes and macrophages by MPO staining confirmed a higher infiltration of liver tissue by immune cells in the absence of Rac1 (Figure 6B). Keeping in mind that MPO expressing cells are recruited to sites of inflammation where they are needed for the removal of apoptotic cells, the data point to aggravated inflammatory and apoptotic processes following DEN treatment especially under situation of Rac1 deficiency. This assumption is in line with the higher frequency of apoptotic cells observed in *rac1* deficient animals 72 h after exposure (Figure 5C). Protein expression of MPO, soluble TNFα and E-selectin, which is an endothelial cell adhesion molecule, was further examined by western blot analysis. The results show that DEN causes a similar increase in the protein expression of these factors in WT and *rac1* KO animals (Figure 6C). Altogether, the results of our studies provide *in vivo* evidence that the small GTPase Rac1 plays a key role in the regulation of multiple DEN-inducible stress pathways that affect DNA repair, DDR, cell cycle progression, cell death and inflammation. Although our analyses clearly demonstrate a considerable influence of Rac1 on both early DEN-stimulated hepatic stress responses and late hepatocarcinogenesis, it remains unclear which of the highly complex effects of Rac1 on acute DEN responses is most causal for the formation of liver tumors at late times. In view of the complexity of carcinogenesis, we speculate that the anticarcinogenic effect developing from Rac1 deficiency is multifarious. Bearing in mind that Rac1 is a key regulator of NADPH oxidase activity (75,76), it appears feasible that ROS signaling and/or oxidative DNA damage contributes to DEN carcinogenesis. In this context we would like to note that an increase in antioxidative capacity has been observed after DEN treatment (77) and the antioxidant NAC was found to attenuate hepatocarcinogenesis (78).

In summary, the data show that Rac1 deficiency impacts the formation of liver tumors following DEN treatment. Based on the data, we suggest that the clonal outgrowth of liver tumors is inhibited when Rac1 is missing. The development of small-sized tumors in *rac1* deficient mice is likely independent of Ras signaling as judged from the lack of *p*-ERK expression. Activated ß-catenin signaling seems also not to be crucial for a specific development of Rac1 deficient tumors, as concluded from the lack of GS expression in Rac1 deficient mice and a similar ß-catenin expression in tumors of both WT and KO mice. The reduced average size of tumors in the absence of Rac1 probably depends on a decreased proliferation rate due to a restrained mitotic progression as inferred from the determination of mitotic index and expression of cyclinB1. The reduced nuclear localization of ß-catenin observed in Rac1 deficient tumors may contribute to this phenotype and requires clarification in future studies employing phenobarbital for tumor promotion. Apart from affecting tumor promotion, Rac1 also affects mechanisms related to the process of tumor initiation. This is concluded from that fact that hepatic KO of *rac1* has multiple effects on early

hepatic responses to DEN treatment. Lack of Rac1 augments the DNA damage response, stimulates the expression of DNA repair factors and increases the incidence of TUNEL positive cells following DEN treatment. We therefore hypothesize that the increased DDR in the absence of Rac1 is predominantly pro-apoptotic, thereby leading to an early and preferential elimination of initiated cells. This is in line with the observation of a lower number and reduced size of liver tumors in Rac1 deficient mice. In the presence of WT Rac1 the DEN-induced DDR is mitigated, resulting in a less efficient elimination of initiated cells. Correspondingly, Rac1 signaling contributes to an augmented tumor formation. A model of the complex consequences of *rac1* deficiency on the process of chemical hepatocarcinogenesis triggered by DEN is displayed in Supplementary Figure S6, available at *Carcinogenesis* Online. Taken together, we conclude that WT Rac1 promotes hepatocarcinogenesis by multiple mechanisms, including the inhibition of the DEN-induced activation of the DDR, suppression of apoptotic death of initiated cells and, ultimately, by facilitating the outgrowth of mouse liver tumors by cooperating with the Ras/Raf/ERK pathway.

Supplementary material

Supplementary Tables 1 and 2 and Figures S1–S6 can be found at http://carcin.oxfordjournals.org/

Funding

Deutsche Forschungsgemeinschaft (Fr 1241/8-1).

Acknowlegements

We are very grateful to V.L. Tybulewicz for generously providing us with the Rac1$^{flox/flox}$ mouse strain. We thank L. Schumacher and B. Opgenoorth (HHU, Düsseldorf) as well as G. Nagel (JGU, Mainz) for excellent technical assistance and R. Ahmadian (HHU Düsseldorf) for providing recombinant Rac proteins (i.e. Rac1, Rac2 and Rac3).

Conflict of Interest Statement: None declared.

References

1. Bokoch, G.M. (2000) Regulation of cell function by Rho family GTPases. Immunol. Res., 21, 139–148.
2. Hall, A. (1998) Rho GTPases and the actin cytoskeleton. Science, 279, 509–514.
3. Schmitz, A.A. et al. (2000) Rho GTPases: signaling, migration, and invasion. Exp. Cell Res., 261, 1–12.
4. Maroto, B. et al. (2008) P21-activated kinase is required for mitotic progression and regulates Plk1. Oncogene, 27, 4900–4908.
5. Halet, G. et al. (2007) Rac activity is polarized and regulates meiotic spindle stability and anchoring in mammalian oocytes. Dev. Cell, 12, 309–317.
6. Mulloy, J.C. et al. (2008) Transforming human blood stem and progenitor cells: a new way forward in leukemia modeling. Cell Cycle, 7, 3314–3319.
7. Mizukawa, B. et al. (2011) Inhibition of Rac GTPase signaling and downstream prosurvival Bcl-2 proteins as combination targeted therapy in MLL-AF9 leukemia. Blood, 118, 5235–5245.
8. Walmsley, M.J. et al. (2003) Critical roles for Rac1 and Rac2 GTPases in B cell development and signaling. Science, 302, 459–462.
9. Wells, C.M. et al. (2004) Rac1-deficient macrophages exhibit defects in cell spreading and membrane ruffling but not migration. J. Cell Sci., 117, 1259–1268.
10. Khosravi-Far, R. et al. (1995) Activation of Rac1, RhoA, and mitogen-activated protein kinases is required for Ras transformation. Mol. Cell. Biol., 15, 6443–6453.
11. Minden, A. et al. (1995) Selective activation of the JNK signaling cascade and c-Jun transcriptional activity by the small GTPases Rac and Cdc42Hs. Cell, 81, 1147–1157.
12. Coso, O.A. et al. (1995) The small GTP-binding proteins Rac1 and Cdc42 regulate the activity of the JNK/SAPK signaling pathway. Cell, 81, 1137–1146.
13. Canman, C.E. et al. (1996) Three paths to stress relief. Nature, 384, 213–214.
14. Jefferies, C.A. et al. (2000) Rac1 regulates interleukin 1-induced nuclear factor kappaB activation in an inhibitory protein kappaBalpha-independent manner by enhancing the ability of the p65 subunit to transactivate gene expression. J. Biol. Chem., 275, 3114–3120.
15. Ungefroren, H. et al. (2011) Differential roles of Smad2 and Smad3 in the regulation of TGF-β1-mediated growth inhibition and cell migration in pancreatic ductal adenocarcinoma cells: control by Rac1. Mol. Cancer, 10, 67.
16. Ellenbroek, S.I. et al. (2007) Rho GTPases: functions and association with cancer. Clin. Exp. Metastasis, 24, 657–672.
17. Liao, J.K. et al. (2005) Pleiotropic effects of statins. Annu. Rev. Pharmacol. Toxicol., 45, 89–118.
18. Inano, H. et al. (1997) Anti-carcinogenic activity of simvastatin during the promotion phase of radiation-induced mammary tumorigenesis of rats. Carcinogenesis, 18, 1723–1727.
19. Narisawa, T. et al. (1994) Prevention of 1,2-dimethylhydrazine-induced colon tumorigenesis by HMG-CoA reductase inhibitors, pravastatin and simvastatin, in ICR mice. Carcinogenesis, 15, 2045–2048.
20. Singh, S. et al. (2014) Chemopreventive strategies in hepatocellular carcinoma. Nat. Rev. Gastroenterol. Hepatol., 11, 45–54.
21. Zhou, Q. et al. (2010) Pleiotropic effects of statins - Basic research and clinical perspectives. Circ. J., 74, 818–826.
22. Hamalukic, M. et al. (2011) Rac1-regulated endothelial radiation response stimulates extravasation and metastasis that can be blocked by HMG-CoA reductase inhibitors. PLoS One, 6, e26413.
23. Heid, I. et al. (2011) Early requirement of Rac1 in a mouse model of pancreatic cancer. Gastroenterology, 141, 719–730, 730.e1–7.
24. Kissil, J.L. et al. (2007) Requirement for Rac1 in a K-ras induced lung cancer in the mouse. Cancer Res., 67, 8089–8094.
25. Samuel, M.S. et al. (2011) K-Ras mediated murine epidermal tumorigenesis is dependent upon and associated with elevated Rac1 activity. PLoS One, 6, e17143.
26. Wang, Z. et al. (2010) Rac1 is crucial for Ras-dependent skin tumor formation by controlling Pak1-Mek-Erk hyperactivation and hyperproliferation *in vivo*. Oncogene, 29, 3362–3373.
27. Malliri, A. et al. (2002) Mice deficient in the Rac activator Tiam1 are resistant to Ras-induced skin tumours. Nature, 417, 867–871.
28. Sugihara, K. et al. (1998) Rac1 is required for the formation of three germ layers during gastrulation. Oncogene, 17, 3427–3433.
29. Kellendonk, C. et al. (2000) Hepatocyte-specific expression of Cre recombinase. Genesis, 26, 151–153.
30. Postic, C. et al. (2000) DNA excision in liver by an albumin-Cre transgene occurs progressively with age. Genesis, 26, 149–150.
31. Vesselinovitch, S.D. (1990) Perinatal mouse liver carcinogenesis as a sensitive carcinogenesis model and the role of the sex hormonal environment in tumor development. Prog. Clin. Biol. Res., 331, 53–68.
32. Rignall, B. et al. (2011) Tumor formation in liver of conditional β-catenin-deficient mice exposed to a diethylnitrosamine/phenobarbital tumor promotion regimen. Carcinogenesis, 32, 52–57.
33. Hatayama, I. et al. (1993) Sex-dependent expression of class pi glutathione S-transferase during chemical hepatocarcinogenesis in B6C3F1 mice. Carcinogenesis, 14, 537–538.
34. Fritz, G. et al. (2011) Potential use of HMG-CoA reductase inhibitors (statins) as radioprotective agents. Br. Med. Bull., 97, 17–26.
35. Briegert, M. et al. (2007) Change in expression of MGMT during maturation of human monocytes into dendritic cells. DNA Repair (Amst)., 6, 1255–1263.
36. Olive, P.L. (2004) Detection of DNA damage in individual cells by analysis of histone H2AX phosphorylation. Methods Cell Biol., 75, 355–373.
37. Aydinlik, H. et al. (2001) Selective pressure during tumor promotion by phenobarbital leads to clonal outgrowth of beta-catenin-mutated mouse liver tumors. Oncogene, 20, 7812–7816.

38. Fritz, G. et al. (1999) Rho GTPases are over-expressed in human tumors. Int. J. Cancer, 81, 682–687.
39. Schnelzer, A. et al. (2000) Rac1 in human breast cancer: overexpression, mutation analysis, and characterization of a new isoform, Rac1b. Oncogene, 19, 3013–3020.
40. Loeppen, S. et al. (2002) Overexpression of glutamine synthetase is associated with beta-catenin-mutations in mouse liver tumors during promotion of hepatocarcinogenesis by phenobarbital. Cancer Res., 62, 5685–5688.
41. Cadoret, A. et al. (2002) New targets of beta-catenin signaling in the liver are involved in the glutamine metabolism. Oncogene, 21, 8293–8301.
42. Zhu, G. et al. (2012) A Rac1/PAK1 cascade controls β-catenin activation in colon cancer cells. Oncogene, 31, 1001–1012.
43. Buongiorno, P. et al. (2008) Rac1 GTPase and the Rac1 exchange factor Tiam1 associate with Wnt-responsive promoters to enhance beta-catenin/TCF-dependent transcription in colorectal cancer cells. Mol. Cancer, 7, 73.
44. Wu, X. et al. (2008) Rac1 activation controls nuclear localization of beta-catenin during canonical Wnt signaling. Cell, 133, 340–353.
45. Howard, S. et al. (2011) A positive role of cadherin in Wnt/β-catenin signalling during epithelial-mesenchymal transition. PLoS One, 6, e23899.
46. Audard, V. et al. (2008) Impaired E-cadherin expression and glutamine synthetase overexpression in solid pseudopapillary neoplasm of the pancreas. Pancreas, 36, 80–83.
47. Akhtar, N. et al. (2001) RAC1 regulates adherens junctions through endocytosis of E-cadherin. Mol. Biol. Cell, 12, 847–862.
48. Takaishi, K. et al. (1997) Regulation of cell-cell adhesion by rac and rho small G proteins in MDCK cells. J. Cell Biol., 139, 1047–1059.
49. Izumi, G. et al. (2004) Endocytosis of E-cadherin regulated by Rac and Cdc42 small G proteins through IQGAP1 and actin filaments. J. Cell Biol., 166, 237–248.
50. Woodcock, S.A. et al. (2010) Tiam1-Rac signaling counteracts Eg5 during bipolar spindle assembly to facilitate chromosome congression. Curr. Biol., 20, 669–675.
51. Harper, J.W. et al. (2007) The DNA damage response: ten years after. Mol. Cell, 28, 739–745.
52. Kinner, A. et al. (2008) Gamma-H2AX in recognition and signaling of DNA double-strand breaks in the context of chromatin. Nucleic Acids Res., 36, 5678–5694.
53. Rogakou, E.P. et al. (1998) DNA double-stranded breaks induce histone H2AX phosphorylation on serine 139. J. Biol. Chem., 273, 5858–5868.
54. Ward, I.M. et al. (2001) Histone H2AX is phosphorylated in an ATR-dependent manner in response to replicational stress. J. Biol. Chem., 276, 47759–47762.
55. Cheng, Q. et al. (2010) Mechanism of p53 stabilization by ATM after DNA damage. Cell Cycle, 9, 472–478.
56. Christmann, M. et al. (2006) c-Fos is required for excision repair of UV-light induced DNA lesions by triggering the re-synthesis of XPF. Nucleic Acids Res., 34, 6530–6539.
57. Christmann, M. et al. (2003) Mechanisms of human DNA repair: an update. Toxicology, 193, 3–34.
58. Kaina, B. et al. (2007) MGMT: key node in the battle against genotoxicity, carcinogenicity and apoptosis induced by alkylating agents. DNA Repair (Amst)., 6, 1079–1099.
59. Chowdhury, G. et al. (2012) Oxidation of methyl and ethyl nitrosamines by cytochrome P450 2E1 and 2B1. Biochemistry, 51, 9995–10007.
60. Bopp, A. et al. (2013) Rac1 modulates acute and subacute genotoxin-induced hepatic stress responses, fibrosis and liver aging. Cell Death Dis., 4, e558.
61. Boehm, J.E. et al. (1999) Rac-dependent anti-apoptotic signaling by the insulin receptor cytoplasmic domain. J. Biol. Chem., 274, 28632–28636.
62. Lorès, P. et al. (1997) Enhanced apoptosis in the thymus of transgenic mice expressing constitutively activated forms of human Rac2GTPase. Oncogene, 15, 601–605.
63. Genot, E.M. et al. (2000) The T-cell receptor regulates Akt (protein kinase B) via a pathway involving Rac1 and phosphatidylinositide 3-kinase. Mol. Cell. Biol., 20, 5469–5478.
64. Burgering, B.M. (2008) A brief introduction to FOXOlogy. Oncogene, 27, 2258–2262.
65. Medema, R.H. et al. (2000) AFX-like Forkhead transcription factors mediate cell-cycle regulation by Ras and PKB through p27kip1. Nature, 404, 782–787.
66. Konstandi, M. et al. (2013) Sex steroid hormones regulate constitutive expression of Cyp2e1 in female mouse liver. Am. J. Physiol. Endocrinol. Metab., 304, E1118–E1128.
67. Tsai, W.B. et al. (2008) Functional interaction between FOXO3a and ATM regulates DNA damage response. Nat. Cell Biol., 10, 460–467.
68. Min, L. et al. (2012) Liver cancer initiation is controlled by AP-1 through SIRT6-dependent inhibition of survivin. Nat. Cell Biol., 14, 1203–1211.
69. Moore, K.A. et al. (1997) Rac1 is required for cell proliferation and G2/M progression. Biochem. J., 326 (Pt 1), 17–20.
70. Hans, F. et al. (2001) Histone H3 phosphorylation and cell division. Oncogene, 20, 3021–3027.
71. Joneson, T. et al. (1996) RAC regulation of actin polymerization and proliferation by a pathway distinct from Jun kinase. Science, 274, 1374–1376.
72. Lamarche, N. et al. (1996) Rac and Cdc42 induce actin polymerization and G1 cell cycle progression independently of p65PAK and the JNK/SAPK MAP kinase cascade. Cell, 87, 519–529.
73. Olson, M.F. et al. (1995) An essential role for Rho, Rac, and Cdc42 GTPases in cell cycle progression through G1. Science, 269, 1270–1272.
74. Coniglio, S.J. et al. (2001) Rac1 protects epithelial cells against anoikis. J. Biol. Chem., 276, 28113–28120.
75. Cheng, G. et al. (2006) Nox1-dependent reactive oxygen generation is regulated by Rac1. J. Biol. Chem., 281, 17718–17726.
76. Hordijk, P.L. (2006) Regulation of NADPH oxidases: the role of Rac proteins. Circ. Res., 98, 453–462.
77. Vo, T.K. et al. (1988) Analysis of antioxidant defense systems during rat hepatocarcinogenesis. Carcinogenesis, 9, 2009–2013.
78. Lin, H. et al. (2013) Antioxidant N-acetylcysteine attenuates hepatocarcinogenesis by inhibiting ROS/ER stress in TLR2 deficient mouse. PLoS One, 8, e74130.